Proc. Natl. Acad. Sci. USA
Vol. 96, pp. 179–184, January 1999
Genetics

Polyglutamine-mediated dysfunction and apoptotic death of a *Caenorhabditis elegans* sensory neuron

PETER W. FABER*†‡, JANET R. ALTER*†‡, MARCY E. MACDONALD§, AND ANNE C. HART*†¶

*Cancer Center and §Molecular Neurogenetics Unit, Massachusetts General Hospital East, and †Department of Pathology, Harvard Medical School, Charlestown, MA 02129

Edited by H. Robert Horvitz, Massachusetts Institute of Technology, Cambridge, MA, and approved November 6, 1998 (received for review August 21, 1998)

ABSTRACT **The effect of expressing human huntingtin fragments containing polyglutamine (polyQ) tracts of varying lengths was assessed in *Caenorhabditis elegans* ASH sensory neurons in young and old animals. Expression of a huntingtin fragment containing a polyQ tract of 150 residues (Htn-Q150) led to progressive ASH neurodegeneration but did not cause cell death. Progressive cell death and enhanced neurodegeneration were observed in ASH neurons that coexpressed Htn-Q150 and a subthreshold dose of a toxic OSM-10::green fluorescent protein (OSM-10::GFP) fusion protein. Htn-Q150 huntingtin protein fragments formed protein aggregates in ASH neurons, and the number of ASH neurons containing aggregates increased as animals aged. ASH neuronal cell death required *ced-3* caspase function, indicating that the observed cell death is apoptotic. Of interest, *ced-3* played a critical role in Htn-Q150-mediated neurodegeneration but not in OSM10::GFP-mediated ASH neurodegeneration. *ced-3* function was important but not essential for the formation of protein aggregates. Finally, behavioral assays indicated that ASH neurons, coexpressing Htn-Q150 and OSM10::GFP, were functionally impaired at 3 days before the detection of neurodegeneration, cell death, and protein aggregates.**

Huntington's disease (HD) is a dominantly inherited, progressive neurodegenerative human disorder caused by pathological expansion of a CAG repeat, encoding polyglutamine (polyQ), in the HD gene (1). HD pathology is restricted to the central nervous system, despite widespread expression of huntingtin (2), and results in progressive brain atrophy as well as selective neuronal cell loss, particularly in the striatum and deep layers of the frontal cortex (3, 4). The length of the mutant CAG repeat correlates with age of neurological onset with typical HD alleles of 40–50 codons leading to midlife onset of the disease (1, 5). In addition to HD, seven other dominant polyQ neurodegenerative diseases have been identified, including spinobulbar muscular atrophy (6), dentatorubropallidoluysian atrophy (7), and several spinocerebellar ataxias (spinocerebellar ataxia 1,2,3,6,7) (8–14). Because the proteins encoded by these loci share no structural similarity outside the polyQ tract (15), the polyQ tract itself has been implicated in driving the disease process with a modulatory role for protein context.

Although the pathogenic mechanism of HD and the other polyQ-mediated diseases is unknown, polyQ expansion alters the physical properties of the mutant huntingtin, as evidenced by decreased mobility on SDS/PAGE and increased reactivity with specific monoclonal reagents (16, 17). Aberrant behavior of mutant huntingtin also results in the formation of cytoplasmic aggregates and intranuclear inclusion bodies in HD brains (18). Intranuclear inclusion bodies contain N-terminally truncated fragments of huntingtin, based on antibody studies. Recently, *in vitro* evidence for a "toxic fragment" model of HD has been obtained. A mouse model partially replicating HD was described by using the promoter and exon 1 of the HD gene with repeat lengths of 115–160 codons (19). A progressive neurological phenotype was obtained without obvious neuropathology in young animals, and intranuclear inclusion bodies, containing the huntingtin fragment, were observed during postmortem examination (20, 21). The same exon 1 protein fragment with an expanded repeat has the ability to aggregate *in vitro* (22). In cell culture models, altered localization and aggregate formation is associated with progressive truncation of the huntingtin protein to small N-terminal fragments containing large expanded polyQ tracts (23–26).

We have begun to address the pathways of cellular dysfunction and death mediated by mutant huntingtin in a genetic system, the nematode *Caenorhabditis elegans*. The effects of pathogenic and control huntingtin fragments on the structure and function of ASH sensory neurons are studied. These neurons mediate behavior in response to various noxious stimuli, including nose touch, high osmolarity, and volatile repellants. The morphology, function, and survival of the ASH neurons is assessed by using a combination of vital dyes, immunohistochemical reagents, and behavioral assays (27–30).

MATERIALS AND METHODS

Plasmid Constructs. The *osm-10* promoter containing plasmid pKP#52 was generated by insertion of a genomic fragment (*Pst*I-*Bam*HI) from cosmid T20H4 (GenBank accession no. U00037, bp 12,848–13,892) in the polylinker of pPD95.67 (31) (see website: file://ciw2.ciwemb.edu/pub/FireLabVectors). Two complementary oligonucleotides (ah90: 5′-GATC*GATATC*GCGGCCGC*GTCGAC*GA-3′ and ah91: 5′-GATCTC*GTCGAC*GCGGCCGC*GATATC*C-3′) containing *Eco*RV and *Sal*I sites (italicized) were inserted in the pKP#52 polylinker *Bam*HI site, generating pHA#13. Comparable *Nco*I-*Xho*I fragments encoding the amino terminal 171 amino acids of huntingtin (GenBank accession no. L13292) with polyQ tracts of 2, 23, 95, and ≈150 residues were inserted between the pHA#13 *Eco*RV and *Sal*I polylinker sites, generating pHA#14 (Q23), pHA#15 (Q95), pHA#16 (Q150), and pHA#22 (Q2). A Xba-linker (Stratagene), introducing a translational stop codon, was inserted in the *Stu*I site immediately preceding the polyQ tract in pHA#16, creating pHA#56. pKP#58, expressing the OSM-10::green fluorescent protein (OSM-10::GFP) fusion protein using the *osm-10* gene

The publication costs of this article were defrayed in part by page charge payment. This article must therefore be hereby marked "*advertisement*" in accordance with 18 U.S.C. §1734 solely to indicate this fact.

This paper was submitted directly (Track II) to the *Proceedings* office.
Abbreviations: HD, Huntington's disease; GFP, green fluorescent protein; DiD, 1,1′-dioctadecyl-3,3,3′,3′-tetramethylindodicarbocyanine perchlorate.
‡P.W.F. and J.R.A. contributed equally to this work.
¶To whom reprint requests should be addressed at: Cancer Center, Massachusetts General Hospital East, Building 149-7202, Charlestown, MA 02129. e-mail: hart@helix.mgh.harvard.edu.

promoter, has been described (A.C.H., J. Kass, J. E. Shapiro, and J. M. Kaplan, unpublished work).

Transgenics. *Transgenic lines*. Transgenic animals were generated by using standard techniques (32) by injection of DNA pools containing constructs of interest and a *dpy-20* rescue construct into the gonads of *dpy-20*(*e1282*) animals (33). Standard DNA concentrations were 125 ng/μl for the dpy-20 rescue plasmid, 75 ng/μl for the huntingtin expression plasmids, and 30 ng/μl for pKP#58. A minimum of three (preferably five) independent lines were selected and analyzed for each DNA pool. The role of *ced-3* function was analyzed by crossing individual arrays into MT5729 (*dpy-20(e1282) unc-30(e191) ced-3(n717) IV*). To avoid misinterpretations of array effects in the *ced-3* mutant background because of survival of the ASI sister neuron, part of the neurons were scored in ignorance of extrachromosomal array present. Animals were transferred to fresh bacterial lawns every (other) day in aging experiments.

Analysis of Transgenic Animals. *Dye filling.* Animals were incubated for 1 hr in 100 ng/μl 1,1′-dioctadecyl-3,3,3′,3′-tetramethylindodicarbocyanine perchlorate (DiD) (34) (Molecular Probes). After destaining for 15 min to 1 hr on fresh bacterial lawns, animals were assayed for DiD uptake and GFP expression (when appropriate) by using an Axoplan2 microscope (Kramer Scientific, Burlington, MA). For each construct, a minimum of 150 ASH neurons were analyzed, except as noted. The percent of dye-filling defective ASH neurons reported represents the average of the dye-filling defect for the corresponding transgenic lines. Because the ASI, PHA, and PHB neurons gave less reproducible dye filling results in wild-type animals, they were excluded from these studies.

Antibody studies. HP1 (35) (1:1,000 dilution) and an anti-GFP mAb (1:500 dilution, CLONTECH) were used to detect the huntingtin fragments and the OSM-10::GFP fusion protein, respectively, in whole mount animals fixed with Bowin's (36). An OSM-10 antisera (A.C.H., J. Kaas, J. E. Shapiro, and J. M. Kaplan, unpublished work) was used to confirm the death of the ASH neurons. To avoid the possibility of misinterpretation because of antibody penetration difficulties, we required positive staining for both ASI neurons and the contralateral ASH neuron before an ASH neuron was scored as absent in immunohistochemical experiments. Because the animals are intrinsically mosaic and the ASI expresses OSM-10 at lower levels than the ASH, this criterion will result in an underestimate of the actual percentage of dead cells of ≈50%. Images were captured by using a SenSys2 camera (Photometrics) and were processed by using IMAGEPRO (Media Cybernetics, Silver Spring, MD) and OPENLAB (Improvisions, Coventry, U.K.) image-analysis software. Confocal resolution was obtained by optical sectioning and a deconvolution program. Because of the nonspecific background of the huntingtin antisera used, we were unable to unambiguously identify the ASH without GFP coexpression. In addition, detection of the huntingtin fragments by Western blotting failed, likely because of the limited *osm-10* expression pattern.

Behavioral assays. Nose touch assays were performed as described (29, 34). The percent of trials in which animals responded to touch by stopping forward movement or reversing is reported.

RESULTS

Htn-Q150 Expression Caused a Dye-Filling Defect in ASH Neurons of 8-Day-Old Animals. Huntingtin fragments containing 2 (Htn-Q2), 23 (Htn-Q23), 95 (Htn-Q95) and ≈150 (Htn-Q150) residues were expressed in *C. elegans* by using the *osm-10* gene promoter (Fig. 1). The *osm-10* gene is expressed in four classes of bilateral sensory neurons, ASH, ASI, PHA, and PHB (Fig. 1; A.C.H., J. Kaas, J. E. Shapiro, and J. M. Kaplan, unpublished work). The sensory endings of these and several other *C. elegans* neurons are exposed to the environment and allow the neurons to take up lipophilic vital dyes, including fluorescein isothiocyanate or DiD. These fluorescent compounds accumulate in cellular membranes, allowing rapid visualization of these cells (Fig. 1); neurons that fail to take up the dye are either absent or have defective sensory endings (37, 38). The vital dye DiD stains all neurons that express OSM-10 as well as four other classes of neurons (Fig. 1). The effect of the huntingtin fragments on ASH staining with DiD (dye filling) was examined in 3-day-old and 8-day-old transgenic animals (Table 1). At 8 days, Htn-Q150 led to a 13 ± 4% dye-filling defect in the ASH neurons. No dye-filling defects were observed in neurons that did not express *osm-10*. The inherent mosaicism of the transgenic lines resulted in a modest underestimation of the Htn-Q150 effect [75% of ASH neurons expressed a GFP marker in comparable transgenic lines (data not shown)]. Htn-Q95, Htn-Q23, and Htn-Q2 caused no dye-filling defects. The Htn-Q150 effect depended on protein expression because a comparable construct containing a translational stop codon immediately before the CAG-repeat did not cause ASH neuron dye-filling defects at 8 days. Dye-filling assays cannot discriminate between ASH neuron death or defective ASH sensory endings. Hence, ASH neuron survival was investigated by using an antiserum that recognizes endogenous OSM-10 protein (Fig. 1; A.C.H., J. Kaas, J. E. Shapiro, and J. M. Kaplan, unpublished work). Of the ASH neurons, 98% were present based on OSM-10 immunoreactivity in both Htn-Q150 and control animals. We conclude that expression of Htn-Q150 leads to degeneration or perturbation of the sensory ending of the ASH neuron but not to cell death.

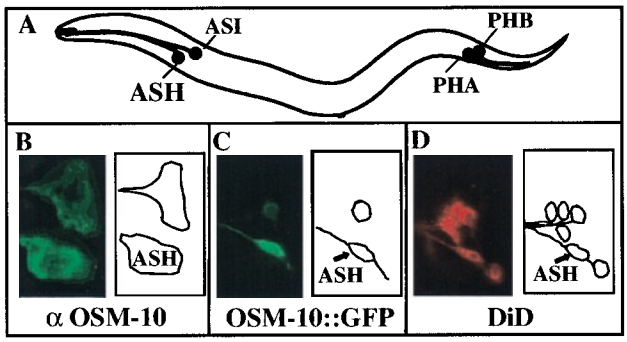

FIG. 1. Overview of the system. (*A*) A schematic presentation of a nematode, indicating the positions of neurons that express the *osm-10* gene. Neurons are referred to by their class designation, e.g., ASHL and ASHR as ASH. (*B*) (Left) ASH and ASI visualized by using the OSM-10 antiserum. (Right) Diagrammed presentation of the stained neurons. (*C*) (Left) ASH and ASI visualized in transgenic animals expressing OSM-10::GFP. (Right) Diagrammed presentation of the stained neurons. (*D*) (Left) DiD stains six classes of neurons, including the ASH, in the head. (Right) Diagrammed presentation of the stained neurons.

Table 1. Percent ASH neuron dye-filling defects in 3- and 8-day-old transgenic animals

Construct (no. of lines)	3-day-old animals	8-day-old animals
Htn-Q2 (5)	0% (174)	0% (218)
Htn-Q23 (5)	0% (204)	0% (207)
Htn-Q95 (5)	0% (221)	0% (254)
Htn-Q150 (13)	0% (406)	13 ± 4% (578)
Htn-Q150-stop (6)	n.d.	0% (351)

Dye-filling experiments using the indicated transgenic animals were performed as described in *Materials and Methods*. The percentage of ASH neurons defective for DiD staining is reported. The number of ASH neurons scored is in parentheses. SEM also is reported. n.d., not determined.

Htn-Q150 Caused ASH Cell Death and Enhanced Dye-Filling Defects when Coexpressed with Subthreshold Levels of a Second Toxic Protein, OSM-10::GFP. Huntingtin fragments were coexpressed in ASH with a second protein, OSM-10::GFP. OSM-10 is a protein required in ASH for avoidance of high osmolarity via an unknown mechanism (A.C.H., J. Kaas, J. E. Shapiro, and J. M. Kaplan, unpublished work). Like endogenous OSM-10, OSM-10::GFP localizes to the cytoplasm of ASH, ASI, PHA, and PHB, but OSM-10::GFP is nonfunctional. Hence, OSM-10::GFP may interfere with the function of OSM-10. High level expression of OSM-10::GFP (but not GFP alone) under control of the *osm-10* promoter caused ASH dye-filling defects. This causally implicates the OSM-10 protein moiety. High level expression of OSM-10::GFP caused a 30 ± 11% ASH neuron dye filling defect at 8 days (three independent lines, 158 ASH neurons scored). A subthreshold level of OSM-10::GFP toxicity was obtained by low level expression, which caused a 1 ± 1% ASH neuron dye-filling defect at 8 days (five independent lines, 225 ASH neurons scored) and was used in all subsequent experiments, unless stated otherwise. Coexpression of huntingtin fragments with OSM-10::GFP allowed rapid discrimination between dye-filling defects and cell death (and avoided underscoring caused by mosaicism). ASH neurons that expressed OSM-10::GFP but failed to dye fill were scored as dye-filling defective; ASH neurons that were dye-filling defective and did not show OSM-10::GFP expression were scored as dead. In these experiments, Htn-Q23 and Htn-Q2 expression caused no defects. Htn-Q95 expression led to dye-filling defects of 5 ± 3% at 8 days (Table 2) but no cell death (Table 3). Htn-Q150 expression led to a 3 ± 1% dye-filling defect at 3 days that increased to 27 ± 6% at 8 days. Importantly, Htn-Q150 expression also led to 2 ± 1% dead cells at 3 days, increasing at 8 days to 11 ± 2% [integration of a Htn-Q150 transgene did not increase the percentage of dead ASH neurons scored (data not shown)]. By using the OSM-10 antisera to confirm ASH cell death, at least 6% of the Htn-Q150 ASH neurons were scored as dead. Dye-filling defective ASH neurons at 8 days were often morphologically distinct. They appeared as "speckled bags," swelling to 2–3 times the size of an unaffected ASH neuron and containing no recognizable intracellular structures as assessed by Nomarski optics (only numerous unidentified faint GFP dots were visible; Fig. 2). Less severely affected ASH neurons also were observed that were swollen but otherwise normal in structure and morphology. Because enhanced toxicity of N-terminal huntingtin fragments might depend on the reduced length of such fragments (23–26), we examined the effect of a shorter N-terminal fragment (Htn-Q150, amino acids 1–79) coexpressed with OSM-10::GFP. This shorter huntingtin fragment caused nearly identical results in dye-filling defects and cell death assays as the longer fragment (data not shown). These experiments indicate that the effects of the huntingtin transgenes on ASH (dye-filling defects and cell death combined) increased with the length of the polyQ tract, with 5% ASH affected at 8 days by Htn-Q95, 5% ASH affected at 3 days by Htn-Q150, and 38% affected at 8 days by Htn-Q150.

Table 2. Percent of ASH neuron dye-filling defects in 3- and 8-day-old transgenic animals

Constructs (no. of lines)	3-day-old animals	8-day-old animals
OSM-10::GFP (5)	0% (163)	1 ± 1% (225)
OSM-10::GFP/Htn-Q2 (5)	0% (168)	0% (203)
OSM-10::GFP/Htn-Q23 (6)	0% (204)	0% (185)
OSM-10::GFP/Htn-Q95 (4)	0% (169)	5 ± 3% (189)
OSM-10::GFP/Htn-Q150 (5)	3 ± 1% (155)	27 ± 6% (235)

Dye-filling experiments, using the specified transgenic animals were performed as described in *Materials and Methods*. The percentage of ASH neurons defective for DiD staining and positive for OSM-10::GFP staining is reported. The number of ASH neurons scored is in parentheses. SEM also is reported.

Table 3. Percent of ASH neuron cell death in 3- and 8-day-old transgenic animals

Constructs (no. of lines)	3-day-old animals	8-day-old animals
OSM-10::GFP (5)	0% (163)	0% (225)
OSM-10::GFP/Htn-Q2 (5)	0% (168)	0% (203)
OSM-10::GFP/Htn-Q23 (6)	0% (204)	0% (185)
OSM-10::GFP/Htn-Q95 (4)	0% (169)	0% (189)
OSM-10::GFP/Htn-Q150 (5)	2 ± 1% (155)	11 ± 2% (235)

Dye-filling experiments using the indicated transgenic animals were performed as described in *Materials and Methods*. The percentage of ASH neurons defective for DiD staining and negative for OSM-10::GFP staining is reported. The number of ASH neurons scored is in parentheses. SEM also is reported.

Htn-Q150 Expression Leads to the Formation of Protein Aggregates. Having established that expression of huntingtin fragments in the ASH led to polyQ-dependent progressive degeneration and death, we used the huntingtin antisera HP1 (35) to visualize and quantify the huntingtin fragments. OSM-10::GFP expression allowed unambiguous identification of the ASH in fixed transgenic animals based on visualization of the GFP marker. Huntingtin fragments were detected at 3 days and 8 days in the cytoplasm and in the sensory and axonal processes of GFP-expressing ASH neurons (Fig. 3.). The percentage of huntingtin immunoreactive ASH neurons and the relative expression levels were comparable for all transgenic lines tested. At 3 days and 8 days, ASH neurons expressing the Htn-Q2 and Htn-Q95 fragments showed diffuse cytoplasmic and process labeling (Fig. 3 *a*, *b*, *d*, and *e*). The Htn-Q150 fragment immunoreactivity was similarly diffuse in 95% of ASH neurons at 3 days (Fig. 3*c*). The remaining 5% of 3-day old Htn-Q150-expressing neurons contained discrete accumulations of huntingtin immunoreactivity, as observed in three independent transgenic lines, *rtEx1*, *rtEx4*, and *rtEx5*. At

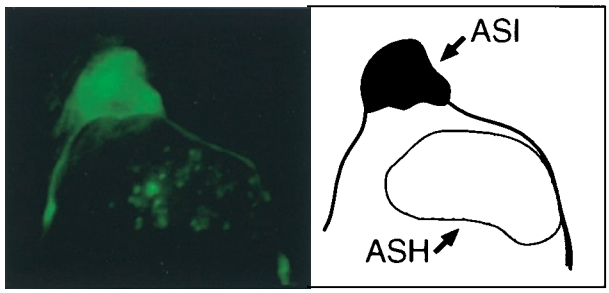

FIG. 2. Htn-Q150/OSM-10::GFP expression led to morphological changes of the ASH in aged animals. (*Left*) An Htn-Q150/OSM-10::GFP-expressing ASH neuron from an 8-day-old animal with a speckled bag phenotype, visualized by GFP fluorescence. Multiple serial section confocal planes were combined for this image. Htn-Q150/OSM-10::GFP expression does not affect the size and morphology of the ASI sensory neurons (as illustrated), and the GFP marker in the ASI neuron shows the normal subcellular expression pattern (A.C.H., J. Kaas, J. E. Shapiro, and J. M. Kaplan, unpublished work). In contrast, a subset of ASH sensory neurons are severely affected, displaying a speckled bag phenotype, swelling to 2–3 times the size of a normal ASH neuron, and lacking intracellular morphology. The subcellular structure, if any, that contains the faint GFP-positive dots is unclear. The size of the ASH and ASI sensory neurons are comparable in wild-type animals. *osm-10* expression in ASH neurons is significantly higher than expression in ASI neurons (A.C.H., J. Kaas, J. E. Shapiro, and J. M. Kaplan, unpublished work), and, consequently, polyQ induced effects are less common in ASI neurons. (*Right*) A schematic representation of the upper panel. The ASI and ASH neurons are outlined.

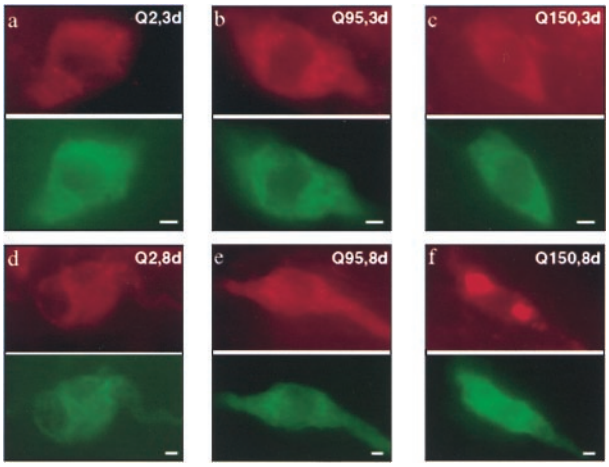

FIG. 3. Htn-Q150 expression led to time-dependent protein aggregation in sensitized ASH neurons. (*a–c Upper*) Visualization of Htn-Q2, Htn-Q95, and Htn-Q150 expression in sensitized ASH sensory neurons in 3-day-old transgenic animals by using the antihuntingtin HP1 (35) antiserum in red. All huntingtin fragments were expressed at similar levels and were found in the cytoplasm and processes without accumulation in obvious intracellular structures. For Htn-Q150, the huntingtin fragments accumulated into discrete foci or aggregates in a very small percentage of the Htn-Q150 expressing ASH sensory neurons (aggregates were found in random locations in the cytoplasm and processes but not in the nucleus, based on visual examination). (*a–c Lower*) The ASH sensory neuron shown in the upper panels visualized with the GFP marker in green. (*d–f Upper*) Visualization of Htn-Q2, Htn-Q95, and Htn-Q150 expression in sensitized ASH sensory neurons in 8-day-old transgenic animals by using the antihuntingtin HP1 (35) antiserum in red. Localization of Htn-Q2 and Htn-Q95 fragments was still broadly cytoplasmic. For Htn-Q150, the huntingtin fragments were detected in large and small cytoplasmic aggregates in over half of the Htn-Q150-expressing ASH neurons. (*d–f Lower*) The ASH sensory neuron shown in the upper panels visualized with the GFP marker in green. (Bar = 3 μm.)

8 days, the number of Htn-Q150-expressing cells with large and small cytoplasmic aggregates had increased 11-fold to 55% for *rtEx1*, *rtEx4*, and *rtEx5* (Fig. 3*f*). These structures were often visible by using Nomarski illumination and visible light. The cytoplasmic aggregates did not contain ubiquitin immunoreactivity. Nuclear inclusions were not detected with HP1 or MAb1 (18) (the huntingtin antisera originally used to immunohistochemically identify nuclear inclusions) at confocal resolution. We concluded that Htn-Q150 expression, but not Htn-Q95 expression, can lead to progressive formation of huntingtin-positive cytoplasmic aggregates.

Htn-Q150 Activates an Apoptotic Cell Death Pathway. Cell death pathways, including programmed cell death (apoptosis), have been well characterized genetically and molecularly in *C. elegans* (39). Loss of function mutations in *ced-3*, a gene encoding a member of the ICE family of cysteine proteases (caspases), prevent developmental apoptosis in *C. elegans.* To address the contribution of apoptosis to Htn-Q150/OSM-10::GFP-mediated cell death, the requirement for *ced-3* function was assessed. An array, *rtEx1*, which caused 10% cell death in *ced-3* (+) animals at 8 days (59 ASH neurons scored) was unable to cause cell death in *ced-3* animals (111 ASH neurons scored). To confirm array integrity, we returned *rtEx1* to a wild-type background, which restores cell death to the original level at 9% (130 ASH neurons scored). Similar *ced-3* suppression was observed for multiple independent transgenic lines by using a second Htn-Q150 construct (A. Gupta, P.W.F., and A.C.H., unpublished work). As described in the previous section, independent expression of either Htn-Q150 or high levels of OSM-10::GFP caused dye-filling defects but not cell death. As a first step toward elucidating the respective roles of Htn-Q150 and OSM10::GFP in ASH cell death, we determined their effect in a *ced-3* mutant background. The dye-filling defect caused by high level OSM-10::GFP expression was independent of *ced-3* function. Two individual OSM-10::GFP expressing extrachromosomal arrays (*rtEx100* and *rtEx101*) caused comparable dye-filling defects in *ced-3* (+) and *ced-3* mutant backgrounds at 8 days (31 ± 20%, 74 ASH neurons scored, and 35 ± 12%, 112 ASH neurons scored, respectively). Returning the arrays to a *ced-3* (+) background caused a similar 32 ± 8% dye-filling defect at 8 days (89 ASH neurons scored). However, examination of the Htn-Q150-mediated dye-filling defect in *ced-3* animals led to a surprising finding. Three individual Htn-Q150-expressing extrachromosomal arrays, (*rtEx102*, *rtEx103*, and *rtEx104*) caused a 30 ± 4% dye-filling defect (117 ASH neurons scored) in *ced-3* (+) animals, but only a 7 ± 1% dye-filling defect (149 ASH neurons scored) in *ced-3* animals at 8 days. To confirm Htn-Q150 array integrity, we returned these arrays to a *ced-3* (+) background, which restored the original dye-filling defect (25 ± 3%, 166 ASH neurons scored).

Next, we quantified the effect *ced-3* function on Htn-Q150-mediated protein aggregation. For *rtEx1* at 8 days, we observed aggregates in 51% of the Htn-Q150-expressing ASH neurons in a wild-type background, in 22% of the Htn-Q150-expressing ASH neurons in *ced-3* mutant animals, and in 59% of Htn-Q150-expressing ASH neurons when *rtEx1* was crossed back in a wild-type background. We conclude that *ced-3* function is required for Htn-Q150-mediated death of ASH neurons that coexpress OSM-10::GFP, plays an important role in the dye-filling defect of ASH neurons that only express Htn-Q150, and plays a role in the formation of the cytoplasmic aggregates in ASH neurons that coexpress OSM-10::GFP.

Htn-Q150 and OSM-10::GFP Coexpression Perturbs ASH Function in Young Animals. Finally, we addressed ASH function in behavioral assays. Wild-type animals stop forward motion and back up in response to nose touch in 70–80% of nose touch trials. Laser ablation of the two bilateral ASH neurons causes a marked decrease in this response to 35% (29). Control and transgenic animals coexpressing Htn-Q150, Htn-Q95, Htn-Q23, and Htn-Q2 with OSM-10::GFP were assayed, as were animals expressing either Htn-Q150 or high levels of OSM-10::GFP, independently. Function of the ASH neurons was unperturbed in animals expressing Htn-Q150 or OSM-10::GFP individually. They responded in >70% of nose touch trials (Fig. 4). Animals expressing either Htn-Q2 or Htn-Q23 in combination with OSM-10::GFP also showed a normal response. In contrast, animals expressing either Htn-

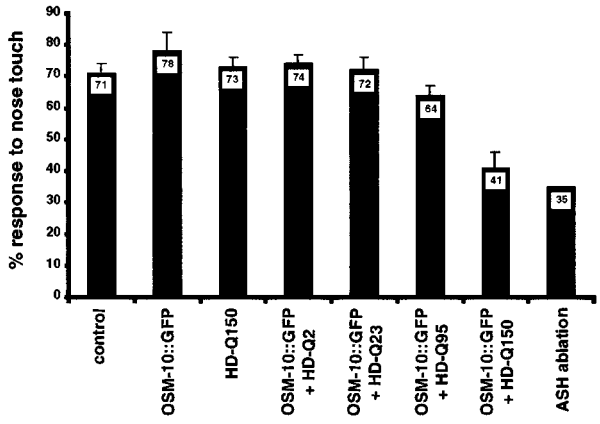

FIG. 4. Htn-Q150 expression in sensitized ASH neurons leads to a severe defect in the nose touch response of transgenic animals. Each bar represents the percentage of trials in which transgenic or control animals (genotype indicated below bar) responded to nose touch by stopping forward movement or reversing. Error bars indicate the SEM). The data for ASH-ablated animals is from Kaplan and Horvitz (29).

Q95 or Htn-Q150 in combination with OSM-10::GFP were defective for ASH-mediated response to nose touch, a modest defect for Htn-Q95 (64 ± 3%) and a pronounced defect for Htn-Q150 (41 ± 5%). We concluded that Htn-Q150/OSM-10::GFP coexpression caused abnormal nose touch response, which approaches the abnormal nose touch response of animals lacking both ASH neurons.

DISCUSSION

Huntington's disease (HD) is one of eight human neurodegenerative disorders caused by expansion of a CAG repeat encoding a polyQ tract (6, 8–14). The pathogenic mechanism underlying these diseases is poorly understood. To address the mechanism of polyQ-mediated cellular dysfunction and death genetically, we are using the nematode *C. elegans.* The nervous system of *C. elegans* is well characterized, and the organism is amendable to powerful genetic studies. By using the *osm-10* gene promoter, huntingtin fragments were expressed in a limited set of *C. elegans* neurons to study the effects of these fragments at single cell resolution. We focused on the ASH sensory neurons to correlate ASH neuron function, morphology, and survival through the use of behavioral assays and vital dyes/immunohistochemical reagents (27–30).

Four N-terminal huntingtin fragments (Htn-Q2, Htn-Q23, Htn-Q95, and Htn-Q150) were expressed in the ASH sensory neurons, alone or in combination with subthreshold levels of a second toxic transgene, OSM-10::GFP. When expressed alone, only Htn-Q150 caused a dye filling defect at 8 days. No cell death was observed, nor were the animals defective in a sensitive behavioral assay, nose touch. In combination with OSM-10::GFP the effects were more pronounced and revealed important properties of polyQ-toxicity in *C. elegans*. As in humans, (*i*) the age of onset and severity increased with repeat length (as determined for dye-filling defects and death by Htn-Q95 and Htn-Q150); (*ii*) toxicity is accompanied by the appearance of protein aggregates (as shown for Htn-Q150) and (*iii*) loss of neuronal function precedes physical degeneration (as determined for Htn-Q95 and Htn-Q150 nose touch defects versus their dye-filling defects and cell death). These observations and correlations validate the ASH neurons in *C. elegans* as a model system for analysis of polyQ toxicity.

In *C. elegans*, as in mouse models for either huntingtin fragments (19), full length ataxin-1 (40), an ataxin-3 fragment (41), or a polyQ tract (42), a very long polyQ tract is necessary to generate a phenotype. Similarly, two recent *Drosophila* models used long polyQ tracts for either a fragment of the spinocerebellar ataxia 3 protein (43) or an N-terminal huntingtin fragment (44). Differences in species, time-frame, and expression levels to cell-type used could explain the requirement for these long tracts in model systems versus the human diseases. To study the effects of the huntingtin fragments on additional *C. elegans* cell types, we performed a preliminary analysis of transgenic animals expressing huntingtin fragments in all neurons (*unc-119* promoter) or in all cells (*dpy-30* promoter) and observed no overt phenotypes (data not shown). A rapid onset in *C. elegans* may require a second toxic stimulus, such as OSM-10::GFP coexpression. Ectopically expressed N-terminal huntingtin fragments containing expanded polyQ tracts enhanced susceptibility of 293T cells to sublethal levels of tamoxifen (23) and of N2A cells to staurosporine (24). Both tamoxifen and staurosporine are apoptotic agents. The experiments using OSM-10::GFP indicated that the sensitizing agent for enhanced polyQ-toxicity need not be apoptotic *per se*. OSM-10::GFP acts nonapoptotically, as a *ced-3* mutation did not affect the dye-filling defect caused by high level expression of OSM-10::GFP. The fact that unenhanced polyQ-mediated phenotypes were observed in mouse and *Drosophila* models might reflect the longer life-span of these organisms. Currently, the molecular basis of OSM-10::GFP toxicity is being addressed and the effects of various other apoptotic/nonapoptotic agents on Htn-Q150 toxicity are being assessed (B. Westlund, J. Spoerke, P.W.F., and A.C.H., unpublished work).

Apoptotic cell death has been implicated in HD because increased levels of DNA strand breaks, indicative of apoptosis, have been observed in brains of HD patients (45). Although the morphological changes we observed were not indicative of apoptotic cell death in *C. elegans* (46), we addressed the involvement of apoptosis in Htn-Q150/OSM-10::GFP-mediated ASH defects genetically. Although the percentage of ASH cell death is relatively low, we observed that Htn-Q150/OSM10::GFP mediated ASH cell death depends on *ced-3* function. We suggest that Htn-Q150 induces this apoptotic cell death because the ability of Htn-Q150 alone to cause an ASH neuron dye-filling defect at 8 days was significantly reduced in a *ced-3* mutant background. In contrast, the ability of OSM-10::GFP alone to cause an ASH neuron dye-filling defect was unchanged in a *ced-3* mutant background. These results are consistent with the reported involvement of apoptosis in polyQ-mediated cell death in *Drosophila* models based on p35 inhibition of cell death (43) or morphology (44).

The Htn-Q2, Htn-Q95 and Htn-Q150 huntingtin fragments expressed in ASH neurons localize to the cytoplasm. We observed the accumulation of large and small cytoplasmic aggregates for Htn-Q150 with increased age. For Htn-Q95, Htn-Q23, and Htn-Q2, no detectable aggregates were observed, even though expression levels were estimated to be similar to Htn-Q150. Insoluble protein aggregates, either in patient material or in *in vitro* systems, have become a hallmark of polyQ disease after the initial identification of nuclear inclusion bodies in both a mouse model for HD that used exon 1 of the HD gene with a polyQ tract of ≈150 residues and in HD brain patient material (18, 20). It has, however, not been established whether such aggregates are cause or consequence of the disease process. The fact that Htn-Q95 led to a minor nose touch defect at 3 days without detectable protein aggregates and the Htn-Q150 led to a major nose touch defect at 3 days with minor aggregation suggests that cellular dysfunction may precede the formation of protein aggregates and may precede dye-filling defects and cell death.

Htn-Q150 and OSM10::GFP co-expression severely impaired the ability of the animal to respond in the nose touch assay. Nose touch is detected by three classes of sensory neurons (ASH, OLQ, FLP), and removal of both ASH neurons in an animal by laser microsurgery eliminates roughly two-thirds of the ability to respond to nose touch (29). Of importance, ablation of one ASH neuron does not impair nose touch response. The 41% residual response we measured suggests that the effect is highly penetrant; given the inherent mosaicism of these transgenic lines, virtually every ASH containing an array is defective in nose touch response. In addition, we tested Htn-Q2/OSM-10::GFP and Htn-Q150/OSM-10::GFP transgenic animals in the less-sensitive osmotic avoidance assay and observed minor defect in Htn-Q150 animals (data not shown). The ASH neurons, therefore, show loss of function before cell death, protein aggregation, or morphological changes occur. This finding mimics observations for HD patients and transgenic mice in which dysfunction and brain atrophy precede detectable cell loss (4, 19).

In summary, by expressing N-terminal huntingtin fragments in ASH sensory neurons, we have generated a model of polyQ-mediated cellular toxicity in *C. elegans* that mimic aspects of the human diseases. Genes/pathways involved in the deleterious effects of expanded polyQ domains on neuronal function can be identified by using genetic approaches and will become immediate targets for analysis of their role in these human diseases. Ultimately, these studies may lead to therapies for the human disorders at early stages in the disease process, preserving function of the afflicted neurons.

The authors would like to thank Cari Hiler and Rachael Moeller for skillful technical assistance, Marian DiFiglia for advice and for generously providing the MAb1 antibody, the *C. elegans* genetic stock center for strains, and members of the Hart and van den Heuvel laboratories for constructive comments and advice. We are indebted to Nancy Bonini, Marty Chalfie, George Jackson, Christian Neri, Gert-Jan van Ommen, Ron Plasterk, and Larry Zipursky for communicating results before publication. The work was supported by the Hereditary Disease Foundation and in part by a Human Science Frontiers Program long-term fellowship to P.W.F. A.C.H. is supported by grants from the Markey Charitable Trust, the Searle Scholar Program, and the Whitehall Foundation.

1. Huntington's Disease Collaborative Research Group (1993) *Cell* **72,** 971–983.
2. Strong, T. V., Tagle, D. A., Valdes, J. M., Elmer, L. W., Boehm, K., Swaroop, M., Kaatz, K. W., Collins, F. S. & Albin, R. L. (1993) *Nat. Genet.* **5,** 259–265.
3. Martin, J. B. & Gusella, J. F. (1986) *N. Engl. J. Med.* **315,** 1267–1276.
4. Vonsattel, J. P., Myers, R. H., Stevens, T. J., Ferrante, R. J., Bird, E. D. & Richardson, E. P., Jr. (1985) *J. Neuropathol. Exp. Neurol.* **44,** 559–577.
5. Gusella, J. F. & MacDonald, M. E. (1995) *Curr. Opin. Neurobiol.* **5,** 656–662.
6. La Spada, A. R., Wilson, E. M., Lubahn, D. B., Harding, A. E. & Fischbeck, K. H. (1991) *Nature (London)* **352,** 77–79.
7. Koide, R., Ikeuchi, T., Onodera, O., Tanaka, H., Igarashi, S., Endo, K., Takahashi, H., Kondo, R., Ishikawa, A., Hayashi, T., *et al.* (1994) *Nat. Genet.* **6,** 9–13.
8. Orr, H. T., Chung, M. Y., Banfi, S., Kwiatkowski, T. J., Jr., Servadio, A., Beaudet, A. L., McCall, A. E., Duvick, L. A., Ranum, L. P. & Zoghbi, H. Y. (1993) *Nat. Genet.* **4,** 221–226.
9. Sanpei, K., Takano, H., Igarashi, S., Sato, T., Oyake, M., Sasaki, H., Wakisaka, A., Tashiro, K., Ishida, Y., Ikeuchi, T., *et al.* (1996) *Nat. Genet.* **14,** 277–284.
10. Pulst, S. M., Nechiporuk, A., Nechiporuk, T., Gispert, S., Chen, X. N., Lopes-Cendes, I., Pearlman, S., Starkman, S., Orozco-Diaz, G., Lunkes, A., *et al.* (1996) *Nat. Genet.* **14,** 269–276.
11. Imbert, G., Saudou, F., Yvert, G., Devys, D., Trottier, Y., Garnier, J. M., Weber, C., Mandel, J. L., Cancel, G., Abbas, N., *et al.* (1996) *Nat. Genet.* **14,** 285–291.
12. Kawaguchi, Y., Okamoto, T., Taniwaki, M., Aizawa, M., Inoue, M., Katayama, S., Kawakami, H., Nakamura, S., Nishimura, M., Akiguchi, I., *et al.* (1994) *Nat. Genet.* **8,** 221–228.
13. Zhuchenko, O., Bailey, J., Bonnen, P., Ashizawa, T., Stockton, D. W., Amos, C., Dobyns, W. B., Subramony, S. H., Zoghbi, H. Y. & Lee, C. C. (1997) *Nat. Genet.* **15,** 62–69.
14. David, G., Abbas, N., Stevanin, G., Durr, A., Yvert, G., Cancel, G., Weber, C., Imbert, G., Saudou, F., Antoniou, E., *et al.* (1997) *Nat. Genet.* **17,** 65–70.
15. Reddy, P. S. & Housman, D. E. (1997) *Curr. Opin. Cell Biol.* **9,** 364–372.
16. Trottier, Y., Lutz, Y., Stevanin, G., Imbert, G., Devys, D., Cancel, G., Saudou, F., Weber, C., David, G., Tora, L., *et al.* (1995) *Nature (London)* **378,** 403–406.
17. White, J. K., Auerbach, W., Duyao, M. P., Vonsattel, J. P., Gusella, J. F., Joyner, A. L. & MacDonald, M. E. (1997) *Nat. Genet.* **17,** 404–410.
18. DiFiglia, M., Sapp, E., Chase, K. O., Davies, S. W., Bates, G. P., Vonsattel, J. P. & Aronin, N. (1997) *Science* **277,** 1990–1993.
19. Mangiarini, L., Sathasivam, K., Seller, M., Cozens, B., Harper, A., Hetherington, C., Lawton, M., Trottier, Y., Lehrach, H., Davies, S. W. & Bates, G. P. (1996) *Cell* **87,** 493–506.
20. Davies, S. W., Turmaine, M., Cozens, B. A., DiFiglia, M., Sharp, A. H., Ross, C. A., Scherzinger, E., Wanker, E. E., Mangiarini, L. & Bates, G. P. (1997) *Cell* **90,** 537–548.
21. Ross, C. A. (1997) *Neuron* **19,** 1147–1150.
22. Scherzinger, E., Lurz, R., Turmaine, M., Mangiarini, L., Hollenbach, B., Hasenbank, R., Bates, G. P., Davies, S. W., Lehrach, H. & Wanker, E. E. (1997) *Cell* **90,** 549–558.
23. Martindale, D., Hackam, A., Wieczorek, A., Ellerby, L., Wellington, C., McCutcheon, K., Singaraja, R., Kazemi-Esfarjani, P., Devon, R., Kim, S. U., *et al.* (1998) *Nat. Genet.* **18,** 150–154.
24. Cooper, J. K., Schilling, G., Peters, M. F., Herring, W. J., Sharp, A. H., Kaminsky, Z., Masone, J., Khan, F. A., Delanoy, M., Borchelt, D. R., *et al.* (1998) *Hum. Mol. Genet.* **7,** 783–790.
25. Hackam, A. S., Singaraja, R., Wellington, C. L., Metzler, M., McCutcheon, K., Zhang, T., Kalchman, M. & Hayden, M. R. (1998) *J. Cell Biol.* **141,** 1097–1105.
26. Li, S. H. & Li, X. J. (1998) *Hum. Mol. Genet.* **7,** 777–782.
27. Hedgecock, E. M., Culotti, J. G., Thomson, J. N. & Perkins, L. A. (1985) *Dev. Biol.* **111,** 158–170.
28. Bargmann, C. I., Thomas, J. H. & Horvitz, H. R. (1990) *Cold Spring Harbor Symp. Quant. Biol.* **55,** 529–538.
29. Kaplan, J. M. & Horvitz, H. R. (1993) *Proc. Natl. Acad. Sci. USA* **90,** 2227–2231.
30. Troemel, E. R., Chou, J. H., Dwyer, N. D., Colbert, H. A. & Bargmann, C. I. (1995) *Cell* **83,** 207–218.
31. Fire, A., Harrison, S. W. & Dixon, D. (1990) *Gene* **93,** 189–198.
32. Mello, C. & Fire, A. (1995) *Methods Cell Biol.* **48,** 451–482.
33. Han, M. & Sternberg, P. W. (1991) *Genes Dev.* **5,** 2188–2198.
34. Hart, A. C., Sims, S. & Kaplan, J. M. (1995) *Nature (London)* **378,** 82–85.
35. Persichetti, F., Ambrose, C. M., Ge, P., McNeil, S. M., Srinidhi, J., Anderson, M. A., Jenkins, B., Barnes, G. T., Duyao, M. P., Kanaley, L., *et al.* (1995) *Mol. Med.* **1,** 374–383.
36. Nonet, M. L., Staunton, J. E., Kilgard, M. P., Fergestad, T., Hartwieg, E., Horvitz, H. R., Jorgensen, E. M. & Meyer, B. J. (1997) *J. Neurosci.* **17,** 8061–8073.
37. Perkins, L. A., Hedgecock, E. M., Thomson, J. N. & Culotti, J. G. (1986) *Dev. Biol.* **117,** 456–487.
38. Starich, T. A., Herman, R. K., Kari, C. K., Yeh, W. H., Schackwitz, W. S., Schuyler, M. W., Collet, J., Thomas, J. H. & Riddle, D. L. (1995) *Genetics* **139,** 171–188.
39. Hengartner, M. O. & Horvitz, H. R. (1994) *Curr. Opin. Genet. Dev.* **4,** 581–586.
40. Burright, E. N., Clark, H. B., Servadio, A., Matilla, T., Feddersen, R. M., Yunis, W. S., Duvick, L. A., Zoghbi, H. Y. & Orr, H. T. (1995) *Cell* **82,** 937–948.
41. Ikeda, H., Yamaguchi, M., Sugai, S., Aze, Y., Narumiya, S. & Kakizuka, A. (1996) *Nat. Genet.* **13,** 196–202.
42. Ordway, J. M., Tallaksen-Greene, S., Gutekunst, C. A., Bernstein, E. M., Cearley, J. A., Wiener, H. W., Dure, L. S. T., Lindsey, R., Hersch, S. M., Jope, R. S., *et al.* (1997) *Cell* **91,** 753–763.
43. Warrick, J. M., Paulson, H. L., Gray-Board, G. L., Bui, Q. T., Fischbeck, K. H., Pittman, R. N. & Bonini, N. M. (1998) *Cell* **93,** 939–949.
44. Jackson, G. R., Salecker, I., Dong, X., Yao, X., Arnheim, N., Faber, P. W., MacDonald, M. E. & Zipursky, S. L. (1998) *Neuron* **21,** 633–642.
45. Dragunow, M., Faull, R. L., Lawlor, P., Beilharz, E. J., Singleton, K., Walker, E. B. & Mee, E. (1995) *Neuroreport* **6,** 1053–1057.
46. Hengartner, M. (1997) in *C. elegans II*, eds. Riddle, D. L., Blumenthal, T., Meyer, B. J. & Preiss, J. R. (Cold Spring Harbor Lab. Press, Plainview, NY), pp. 383–416.